Journal of Power Sources 199 (2012) 132–137

Contents lists available at SciVerse ScienceDirect

Journal of Power Sources

journal homepage: www.elsevier.com/locate/jpowsour

Performance of a commercial cathode-supported solid oxide fuel cells prepared by single-step infiltration of an ion-conducting electrocatalyst

Xue Li, Nansheng Xu, Xuan Zhao, Kevin Huang*

Department of Mechanical Engineering, University of South Carolina, Columbia, SC 29208, United States

ARTICLE INFO

Article history:
Received 28 September 2011
Received in revised form 21 October 2011
Accepted 21 October 2011
Available online 25 October 2011

Keywords:
Infiltration
Ionic conductor
Electrocatalyst
Cathode polarization
Solid oxide fuel cell

ABSTRACT

Infiltration of fine-grained electrocatalyst particles into ceramic porous scaffolds is a very effective way to improve electrode performance for low-to-intermediate temperature solid oxide fuel cells (SOFCs). Conventionally, fine particles of an electronic or mixed electronic and oxide-ion conducting material are impregnated into an ion conducting porous scaffold. However, this approach usually requires higher infiltrant-loading, therefore tedious repetitive infiltration/drying and calcinations steps, in order to form percolated electron conducting network for effective current collection. In this study, we present an alternative single-step route involving infiltration of an ion conducting Sm-doped CeO_2 (SDC) into an electron conducting cathode porous scaffold as well as anode of a commercial cathode-supported SOFC. A comparative study shows that the cathode polarization can be reduced by a factor of five to thirteen from 700 to 1000 °C by the infiltrated SDC. The single-cell performance exhibits a performance improvement by a factor of three from 700 to 800 °C. Stability tests within a limited time frame and low current-density show a relatively flat performance for SDC-infiltrated cell and "break-in" behavior for the baseline cell, suggesting electrolyte/cathode interface being activated by the infiltrated electrocatalyst.

1. Introduction

Cathode-supported solid oxide fuel cell (SOFC) represents one branch of electrode-supported thin-film SOFCs. The performance of a cathode-supported SOFC is, however, inferior to its counterpart anode-supported one, largely due to the fact that co-sintering electrolyte thin-film on perovskite-oxide based cathode substrate invokes deleterious chemical reactions, forming electrically insulating and electrochemically blocking phases at the electrolyte/cathode interface. Therefore, the concept of cathode-supported SOFC is technically not as attractive as anode-supported one in which a better chemical compatibility exists between the two-phase anode substrate and the electrolyte. The cathode-supported SOFC design becomes rational only when it combines with tubular geometry and operating at high temperatures (>900 °C). The advantages of cathode-supported tubular SOFCs have been demonstrated by the outstanding reliability of Siemens' (formerly Westinghouse's) SOFC systems. The unique features such as no-gas-seals, Ni-based cell-to-cell connection scheme in reducing atmospheres, Cr-poisoning-free $LaCrO_3$-based ceramic interconnect and non-constraint bundle/stack design are the principal reasons for the observed remarkable durability [1–3].

The major issue with the cathode-supported tubular SOFC technology is the low power performance, which further translates to a higher cell cost in $/kW. Since the most active cathodes, i.e., Sr- and Fe-doped $LaCoO_3$, are chemically reactive with the electrolyte (i.e., ZrO_2-based) and have appreciably higher thermal expansion coefficients than the electrolyte, materials selection for the cathode substrates is largely confined to those electronic conductors, i.e., doped $LaMnO_3$, which have close thermal expansion match to the electrolyte but poor electrochemical activity to oxygen-molecule reduction. Increasing power density is, therefore, the most desirable task for the development of cathode-supported SOFCs. A common engineering solution to this performance problem without compromising the mechanical integrity is to apply a composite interlayer consisting of electrolyte and cathode phases at the cathode/electrolyte interface [4–6]. Since the properties of thus applied cathode interlayer are largely dictated by the higher temperature densification of the electrolyte, the degree to which the performance can be improved is limited. Therefore, further improvement on the performance of cathode-supported SOFCs by an alternative approach is still very demanding.

Infiltration of electrochemically active fine-grained catalysts into a ceramic porous scaffold is a methodology developed in recent years to enhance electrode performance of SOFCs [7–17]. It was suggested that almost any kind of dopants can, when infiltrated onto the surface of a perovskite film, enhance electrode performance [18]. It has, therefore, spurred a great deal of interests in

* Corresponding author. Tel.: +1 803 777 0204; fax: +1 803 777 0106.
E-mail address: kevin.huang@sc.edu (K. Huang).

0378-7753/$ – see front matter © 2011 Elsevier B.V. All rights reserved.
doi:10.1016/j.jpowsour.2011.10.079

applying this technique to the development of low-to-intermediate temperature SOFCs where electrode polarizations dominate the cell performance. Several comprehensive reviews on this topic can also be found in Ref. [7,19]. Not only can electrode polarization be markedly reduced as a result of the increased surface area of finer particles and improved electrocatalytic activity of better materials, but also this brilliant technique can create an electrode architecture offering excellent electrocatalytic activity while still maintaining good thermal-expansion match to the electrolyte [15]. Independent catalyst calcination step allowing for a better control of particle size and morphology of the infiltrated electrocatalysts is another conceivable advantage [20–22].

Impregnating a mixed ion/electron-conducting or electron-conducting fine-grained perovskite oxides into an ion-conducting electrolyte scaffold is the most commonly practiced infiltration technique [9–17]. However, this process requires many infiltration repetitions of low-concentration nitrate solutions in order to achieve sufficient solid loading and to form percolated electron conduction network [9,12,15]. Infiltrating a precursor solution with too high a concentration would lead to a preferential segregation of the active elements to the sample surface during drying step, causing non-uniform distribution of the desirable phases across the porous scaffold [7,8,23]. Only limited effort has been devoted to developing one-step infiltration with high nitrate concentration in the presence of dispersant [9]. Nevertheless, non-uniform distribution and insufficient loading of electron-conducting catalysts can lead to ineffective network of electron conduction, causing increased ohmic loss for current collection. This current-collection issue can be easily overlooked in laboratory button-cell tests where noble-metal meshes/pastes are embedded in a relatively thin electrode structure serving as the current collector. Significantly increasing catalyst loading can improve electronic conductivity, but it requires tedious infiltration/drying/calcination repetitions and could potentially reduce the original porosity of the porous scaffold, causing problem of gas transport.

Alternatively, the composite nature of good electrode structure can be retained by incorporating ion-conducting electrocatalysts into an electron-conducting porous scaffold. The advantage of this process is that the current-collection can be carried out by the bulk electron-conducting electrode substrate with a minimal ohmic loss. The requirement for a large catalyst loading is, therefore, no longer demanding, which not only simplifies the infiltration process but also preserves the needed porosity in the porous scaffold. Recall that cathode-supported SOFCs to a great extent need performance enhancement. It is, therefore, a sensible approach to infiltrate ion-conducting electrocatalysts for further improvement of the performance.

In this paper, we describe a single-step procedure of infiltrating a Sm-doped CeO_2 (SDC) oxide-ion conducting electrocatalyst into the cathode porous scaffold as well as anode layer of a commercial cathode-supported tubular SOFC. A comparative study on cathode polarization resistance between infiltrated and baseline cell is particularly conducted to illustrate the benefit of the infiltrated electrocatalyst. The performance of a complete commercial cathode-supported tubular SOFC with SDC-infiltrated cathode and anode is also compared.

2. Experimental procedure

2.1. Simplified single-step infiltration of SDC electrocatalyst

The tubular segments of cathode-supported SOFC used in this study are provided by the courtesy of Siemens. The physical dimensions are 22 mm in outer diameter, 18 mm in inner diameter and 20 mm in length. The cathode substrate has an average pore size and porosity of 10 μm and 30%, respectively [6]. The cathode is chemically comprised of 30 mol% Ca and 10 mol% Ce doping on the La-site and minor Ni and Cr doping (<1 mol%) on the Mn-site of $LaMnO_3$ perovskite. The electrolyte layer consists of a 10 mol% Sc and 1 mol% Ce doped ZrO_2 (ScCeSZ), fabricated by atmospheric plasma spraying deposition technique. Details on materials perspective of Siemens' cathode-supported tubular SOFCs can be found in Ref. [6].

The infiltration process used in this study is primarily based on the procedure described in Ref. [9], but with a simplification of how the precursor solution is impregnated into the porous scaffold. A detailed description is given as follows. A solution containing SDC precursor is first prepared by dissolving 8.8893 g $Sm(NO_3)_3{\cdot}6H_2O$ (Alfa Aesar, 99.9% pure) and 34.7376 g $Ce(NO_3)_3{\cdot}6H_2O$ (Alfa Aesar, 99.9% pure), and 1.3088 g surfactant Triton-X100 (3 wt.%, Union Carbide Chemicals and Plastics Co., Inc.) in 39.2 ml DI-H_2O with stirring for more than 1 h. To ensure the right stoichiometry of the starting nitrate precursors, the "Loss-of-Ignition" (LOI) method was used to accurately determine the number of water in the nitrates prior to weighing. The concentration of Sm/Ce in the starting solution is 2 M. Then a tubular segment with a densified electrolyte layer is immersed into the prepared solution, followed by heating it to 80 °C. During the heating, the air trapped in the pores gradually escapes, allowing the precursor solution to fully penetrate deep into the interface of cathode/electrolyte. At the same time, the precursor solution becomes viscous and gradually reaches the nitrate solubility limit. The infiltrated cell is then removed from the solution, dried at room temperature and then 110 °C for a few hours, and finally fired in air at 600 °C for 2 h to decompose the precursor into SDC nanoparticles. For a cell with the anode in place, the same procedure was repeated so that both cathode and anode were filled with SDC nanoparticles simultaneously. Due to the effective loading per infiltration step, no more than single infiltration was needed in either case for the concerns of reduced porosity in the electrode structure. The phase purity and microstructural features of the infiltrated SDC were examined with Rigaku D/max-A X-ray Diffractometer (CuKα radiation) and Zeiss Ultra plus FE-SEM, respectively.

2.2. Comparative study on cathode polarization

The comparative study was conducted on half-cell fashion of cathode-supported SOFC, consisting of only cathode and electrolyte. The thickness of ScCeSZ electrolyte is approximately 60 μm. Platinum was used as the counter electrode (CE). A schematic is given in Fig. 1(a). It is understood that the measured polarization resistance by AC impedance spectroscopy will include contributions from both cathode and Pt-CE, of which only cathode contribution is the interest to this study. However, if a change is only made to the cathode such as infiltration of electrocatalysts, the corresponding change in polarization resistance observed on impedance spectrum should only originate from that change as the Pt-CE remains unchanged. This has become the basis for the comparative study of cathode polarization between infiltrated and baseline cells.

The Pt-CE coating on the electrolyte surface was prepared from a commercial Pt paste (Heraeus CL5100) along with Pt-meshes/leads serving as the current collectors by curing at 800 °C for 30 min. The effective cell surface area was kept at 1 cm^2. The AC impedance measurements were carried out in a flowing air at 100 sccm from 700 to 1000 °C with a Zahner IM6 Electrochemical Workstation.

2.3. Segment cell testing

The schematic of cathode-supported tubular SOFC segment studied is shown in Fig. 1(b). The cell included a 2 mm thick cathode substrate supporting a roughly 60 μm-thick ScCeSZ layer and a 100 μm-thick ScCeSZ/NiO (1:1, v/v) anode. To minimize the

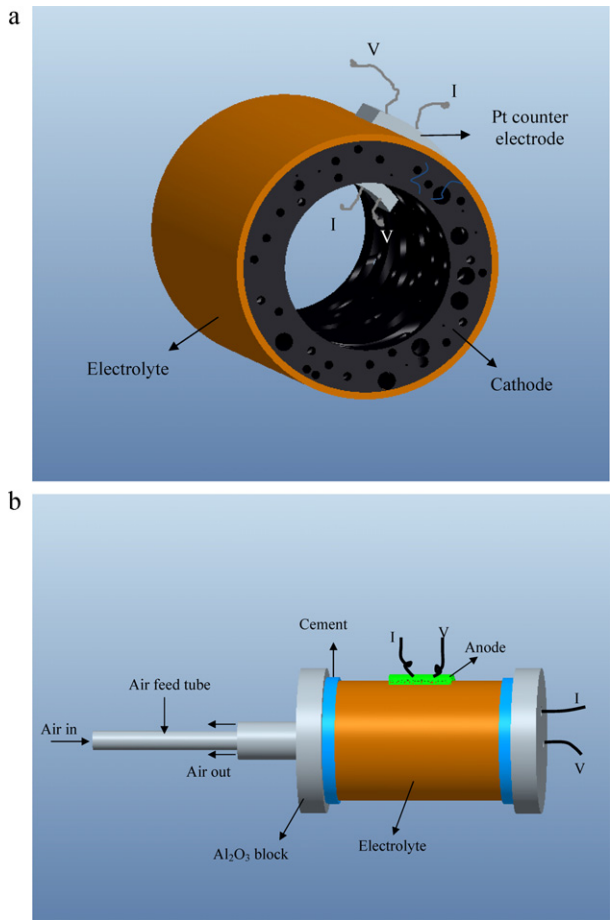

Fig. 1. Cell configurations for comparative studies of electrochemical performance. (a) Half-cell AC impedance spectroscopy study; (b) full-cell electrochemical characterization.

number of variables, the two tube segments for the comparative study were adjacently cut from the same cell. The NiO/ScCeSZ anode layer was coated from an ink made of NiO/ScCeSZ and a commercial binder (Heraeus, V-006) in a weight ratio of 1:2, followed by firing it in air at 1300 °C for 1 h. The NiO in the NiO/SSZ electrode is expected to become Ni after exposure to the H_2-containing atmosphere. The effective cell surface area was 1 cm^2. After the single-step infiltration of SDC into both cathode and anode layer, the cell was sealed with a commercially available cement (Aremco Products. Inc., Ceramabond 552-VFG) and electrochemically tested from 600 to 800 °C with a Zahner IM6 Electrochemical Workstation. The flow rates of air and H_2 (containing 3% H_2O) were set to 100 cc min^{-1} and 40 cc min^{-1}, respectively, for the test.

3. Results and discussion

3.1. Characterization of infiltrated SDC

The phase identity of the prepared SDC after calcining at 600 °C for 2 h is examined with XRD. The result shown in Fig. 2 clearly indicates a pure phase of SDC with fluorite structure although it was yet fully crystallized. This independent checking ensures the formation of the wanted SDC phase present in the cathode porous scaffold. The morphology of the SDC particles after calcining at 600 °C for 2 h is displayed in Fig. 3 by SEM at near the electrolyte/cathode interface. The SDC particles do not appear to form percolated structure, but rather are present as uniformly distributed islands at nano-scale.

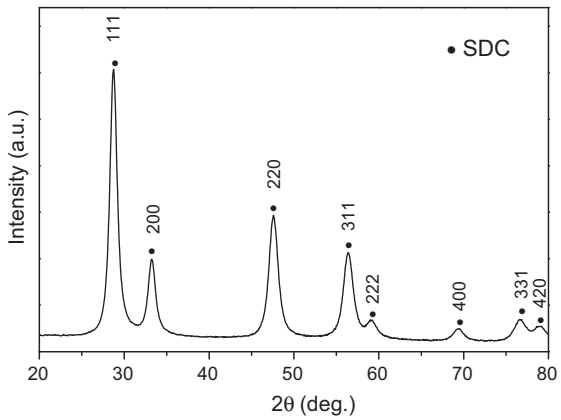

Fig. 2. XRD pattern of the prepared SDC powder.

The slightly higher atomic ratio of Ce/Sm (>4.6:1) as detected by EDS is probably a result from the presence of Ce in the parent substrate.

3.2. Comparative study of cathode polarization

The AC impedance spectra of cathode/electrolyte/Pt cells measured from 700 to 1000 °C under the OCV condition are compared in Fig. 4. The polarization resistance recorded as the length between the high-frequency and the low-frequency intersections with the Z'-axis is substantially reduced by the infiltrated SDC catalysts. In contrast, the ohmic resistance as represented by the high-frequency intersection with Z'-axis remains relatively unaffected. A side-by-side comparison of polarization resistance (including both cathode and Pt-CE in this case) between baseline and SDC infiltrated cells suggests a factor of five to thirteen reductions in the temperature range studied. The observed cathode polarization reduced by the infiltrated SDC is an indirect indication of the activation process of oxygen molecules being the rate-limiting step, which agrees with the previous conclusion that the cathode polarization is the performance-limiting factor for cathode-supported SOFCs [6].

To further understand the role of infiltrated SDC played in cathode kinetics, Arrhenius plots of ohmic (R_{ohm}) and polarization (R_p) area specific resistances of infiltrated and baseline cells are shown in Fig. 5, where straight-lines of both signal thermally activated processes. In particular, no significant difference in R_{ohm} values and activation energy E_a can be discerned in Fig. 5(a). The obtained activation energy E_a = 0.86–0.87 eV also agrees well with that reported value [6]. Similar trend in activation energies for polarization resistance R_p of both cells shown in Fig. 5 (b) are also observed, E_a = 1.92 eV for the baseline cell and 2.07 eV for the infiltrated one. However, there is marked difference in the actual R_p values. This difference is clearly originated from the pre-exponential term in the Arrhenius equation $R_p = R_p^o \exp(E_a/kT)$. Since R_p^o usually decreases with the concentration of active oxygen species or triple phase boundary (TPB) density, one reasonable interpretation of Fig. 5(b) is that the infiltrated SDC discrete particles increase the concentration of active oxygen species or TPB density. This conjecture seems to contradict with conventional theory that requires ion conducting phase to be percolated for getting involved in oxygen reduction reaction (ORR) [24]. However, considering the fact that the ORR only occurs within 10–20 μm thickness of the electrolyte/cathode interface, interconnected SDC phase is not necessary as long as it is present in the electrochemically active region where oxygen molecules, oxide-ions and electrons meet. The known catalytic activity of SDC on ORR, particularly in nano-size scale, would certainly result in lower R_p as observed in this study.

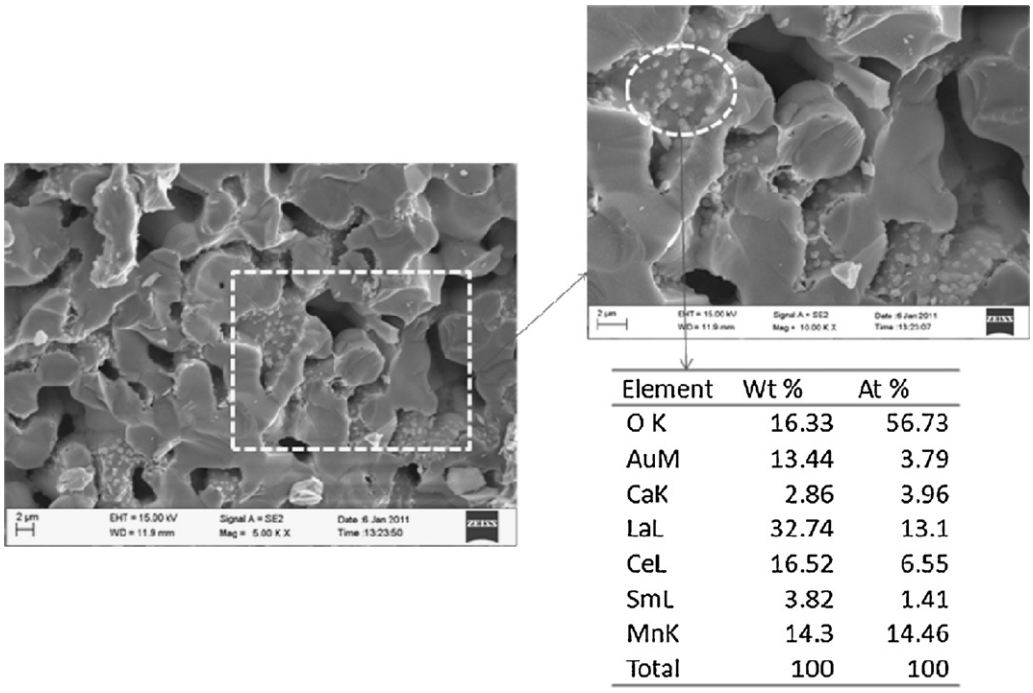

Fig. 3. SEM image and EDS composition of the infiltrated SDC.

3.3. Single segment cell testing

A comparative study was also conducted between the baseline and the SDC-infiltrated SOFC in a complete cell fashion. Fig. 6 shows the AC impedance spectra of the two cells measured at 800 °C under OCV and 100 mA cm^{-2} loading conditions. Again, drastic reduction in cell polarization resistance is observed in the SDC-infiltrated cell. As high as seventeen-fold and seven-fold

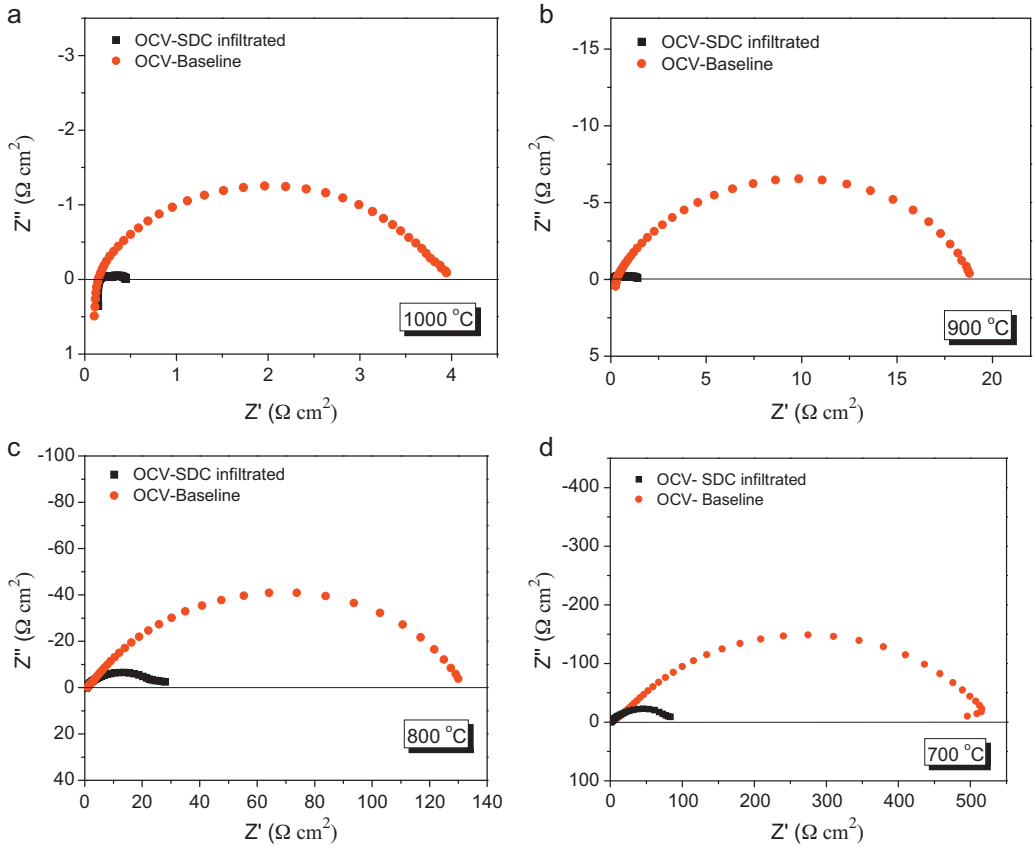

Fig. 4. Comparison of impedance spectra between baseline and SDC-infiltrated half-cells. (a) 1000 °C; (b) 900 °C; (c) 800 °C; (d) 700 °C.

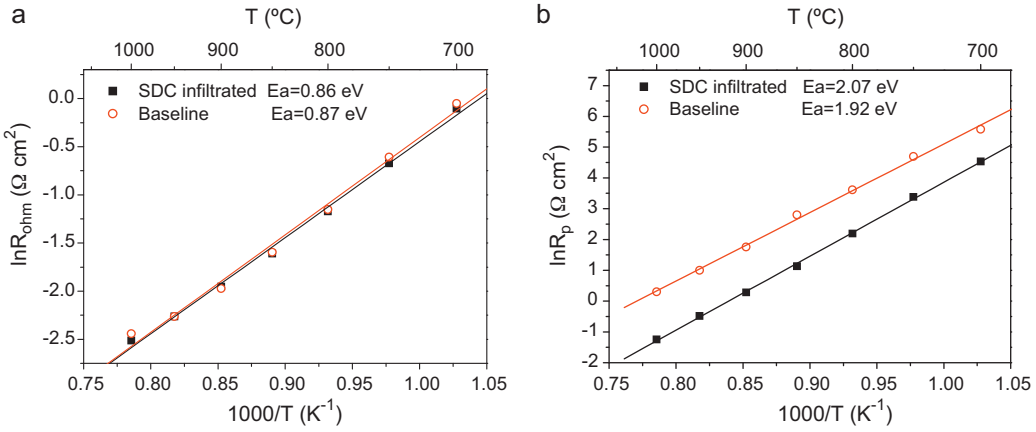

Fig. 5. (a) Arrhenius plots of (a) ohmic resistance and (b) polarization resistance.

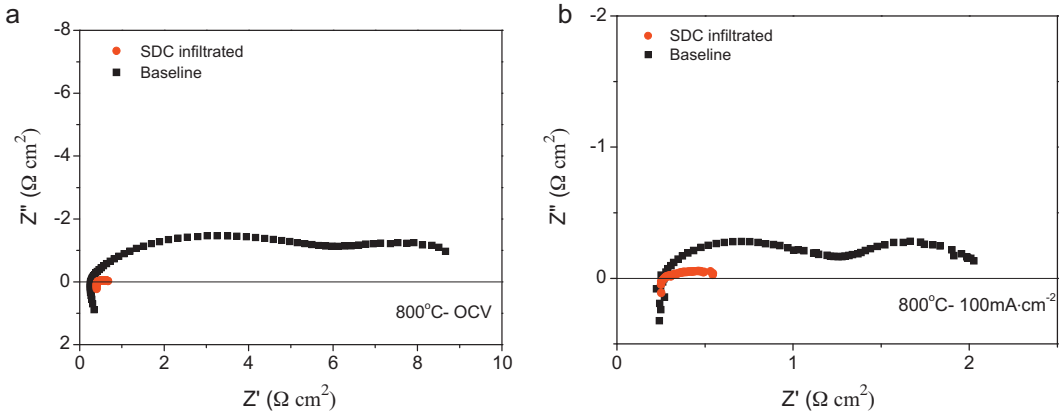

Fig. 6. Comparison of impedance spectra between baseline and SDC-infiltrated full-cells under real SOFC operating conditions. (a) OCV; (b) 100 mA cm^{-2}.

reductions in total electrode polarization are observed for infiltrated cell under OCV and 100 mA cm^{-2} loading, respectively. The lower degree polarization reduction under electrical loading infers that the cathode-supported SOFC can be electrically activated. This electrical activation phenomenon is also closely related to the "break-in" behavior observed in SOFCs [25–28]. In fact, the sensitivity of electrode polarization to electrical loading is another sign of activation polarization (charge-transfer) to be the rate-limiting step as the cathodic current can produce oxygen vacancies at the cathode/electrolyte interface for promoting charge-transfer process. Since the measured spectra include contributions from cathode as well as anode, the observed polarization reductions should be attributed to the one-step infiltration process described above.

The electrical performance of the baseline and SDC-infiltrated cells is compared in Fig. 7. As is well known that the performance of a cathode-supported SOFC is low, particularly in lower temperature range, it is no surprise to see that the peak power density only reached 100 and 50 mW cm^{-2} at 800 and 700 °C, respectively. The performance is largely dominated by the activation polarization as evidenced by the sharp decrease of cell voltage in low current density regime. However, the low performance of baseline cell can be markedly increased by a factor of three to 300 and 180 mW cm^{-2} at 800 and 700 °C, respectively. The cell voltage is essentially linear with current density for the most part of *V–J* curve until a sharp drop in voltage appears at round 0.5 A cm^{-2} (for 800 °C). The rapid drop at higher current density is clearly related to the limited oxygen diffusion in the porous cathode substrate. The magnitude of the limiting current density at which the sharp voltage drop is observed agrees well with that reported in [28–30]. The thick and relatively low-porosity cathode substrate developed by Siemens is an engineering solution to balancing equally important mechanical strength and power performance.

Long-term stability of any infiltrated fine-grained catalysts at elevated temperatures is a major concern to practical applications [10,12,31–33]. Therefore, we also tested, though within a very limited time-frame and low current-density, the stability of infiltrated and baseline cells. The results are shown in Fig. 8. Within the tested hours, the performance of baseline-cell

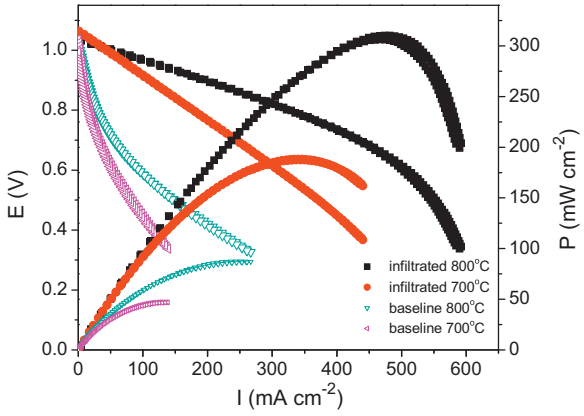

Fig. 7. Comparison of power performance between baseline and SDC-infiltrated SOFCs.

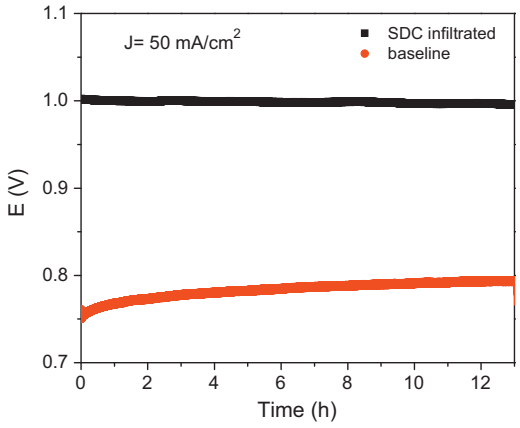

Fig. 8. Stability tests of baseline and SDC-infiltrated cells at 800 °C and 50 mA cm^{-2}.

improved with time, demonstrating the well-known "break-in" behavior as previously reported [25–28]. In contrast, a relatively flat performance is observed for the infiltrated cell. The lack of "break-in" phenomenon observed in the infiltrated cell is an indirect sign of activated electrode/cathode interface by the infiltrated SDC catalyst. However, the true long-term stability of the SDC-infiltrated SOFC needs to be carried out in our future continued research.

4. Conclusions

Fine particles of ion-conducting electrocatalyst SDC have been successfully infiltrated into a commercial cathode porous scaffold as well as anode by a simplified one-step approach. The morphology of the impregnated SDC features discrete nano-particles well-dispersed throughout the cathode substrate. A comparative study shows that the cathode polarization can be substantially reduced by a factor of six to thirteen in the temperature range of 700–1000 °C by the infiltrated SDC nanoparticles. Another comparative study shows that the performance of a normal cathode-supported single cell can be improved by a factor of three with infiltrating SDC into both cathode and anode. Although it is difficult to determine the exact rate-limiting step and mechanisms from this study, the beneficial effect from the infiltrated SDC nano-particles as electrocatalytically active sites for promoting a faster ORR is clearly demonstrated. A stability test within limited time-frame and low current-density reveals noticeable "break-in" behavior of the baseline cell and relative flat performance of the infiltrated cell.

Acknowledgement

The authors would like to thank DARPA (W91CRB-10-1-0007) for financial support.

References

[1] R. George, J. Power Sources 86 (1–2) (2000) 134–139.
[2] R. George, N.F. Bessette, J. Power Sources 71 (1–2) (1998) 131–137.
[3] S.E. Veyo, L.A. Shockling, J.T. Dederer, J.E. Gillett, W.L. Lundberg, J. Eng, Gas Turb. Power 124 (4) (2002) 845.
[4] N.Q. Minh, Solid State Ionics 174 (2004) 271.
[5] J. Mertens, V.A.C. Haanappel, C. Wedershoven, H.-P. Buchkremer, J. Fuel Cell Sci. Technol. 3 (2006) 415.
[6] K. Huang, 7th Euro. SOFC Forum, P0303, Lucerne, Switzerland, 3–7 July 2006, 2006.
[7] J.M. Vohs, R.J. Gorte, Adv. Mater. 21 (2009) 943–956.
[8] P. Jiang, Mater. Sci. Eng. 418 (1–2) (2006) 199–210.
[9] T.Z. Sholklapper, C. Lu, C.P. Jacobson, S.J. Visco, L.C. De Jonghe, Electrochem. Solid-State Lett. 9 (2006) A376.
[10] T.Z. Sholklapper, V. Radmilovic, C.P. Jacobson, S.J. Visco, L.C. De Jonghe, Electrochem. Solid-State Lett. 10 (4) (2007) B74–B76.
[11] T.Z. Sholklapper, H. Kurokawa, C.P. Jacobson, S.J. Visco, L.C. De Jonghe, Nano Lett. 7 (7) (2007) 2136–2141.
[12] W. Wang, M.D. Gross, J.M. Vohs, R.J. Gorte, J. Electrochem. Soc. 154 (2007) B439.
[13] F. Bidrawn, S. Lee, J.M. Vohs, R.J. Gorte, J. Electrochem. Soc. 155 (2008) B660.
[14] J.D. Nicholas, A. Scott, Barnett, J. Electrochem. Soc. 157 (4) (2010) B536–B554.
[15] Y. Huang, J.M. Vohs, R.J. Gorte, Electrochem. Solid-State Lett. 9 (5) (2006) A237–A240.
[16] N. Ai, S.P. Jiang, Z. Lü, K. Chen, W. Su, J. Electrochem. Soc. 157 (7) (2010) B1033–B1039.
[17] R.J. Gorte, J.M. Vohs, Curr. Opin. Colloids Interface Sci. 14 (4) (2009) 236–244.
[18] F. Bidrawn, G. Kim, N. Aramrueang, J.M. Vohs, R.J. Gorte, J. Power Sources 195 (720) (2010).
[19] T.Z. Sholklapper, C.P. Jacobson, S.J. Visco, L.C. De Jonghe, Fuel Cells 5 (2008) 303.
[20] R. Craciun, R.J. Gorte, J.M. Vohs, C. Wang, W.L. Worrell, J. Electrochem. Soc. 146 (1999) 4019.
[21] H. Kim, C. Lu, W.L. Worrell, J.M. Vohs, R.J. Gorte, J. Electrochem. Soc. 149 (2002) A247.
[22] R.J. Gorte, S. Park, J.M. Vohs, C. Wang, Adv. Mater. 12 (2000) 1465.
[23] S. Jung, C. Lu, H.P. He, K. Ahn, R.J. Gorte, J.M. Vohs, J. Power Sources 154 (42) (2006).
[24] D. Gostovic, J.R. Smith, D.P. Kundinger, K.S. Jones, E.D. Wachsman, Electrochem. Solid-State Lett. 10 (12) (2007) B214–B217.
[25] L.F.J. Piper, A.R.H. Preston, S.-W. Cho, A. DeMasi, B. Chen, J. Laverock, K.E. Smith, L.J. Miara, J.N. Davis, S.N. Basu, U. Pal, S. Gopalan, L. Saraf, T. Kaspar, A.Y. Matsuura, P.-A. Glans, J.-H. Guo, J. Electrochem. Soc. 158 (2) (2011) B99–B105.
[26] C. Sun, R. Hui, J. Roller, J. Solid State Electrochem. 14 (7) (2010) 1125–1144.
[27] S.P. Simner, M.D. Anderson, J.W. Stevenson, J. Am. Ceram. Soc. 87 (8) (2004) 1471–1476.
[28] D. Beckel, U.P. Muecke, T. Gyger, G. Florey, A. Infortuna, L.J. Gauckler, Solid State Ionics 178 (40) (2007) 7–415.
[29] K. Huang, J. Electrochem. Soc. 151 (5) (2004) A716–A719.
[30] K. Huang, J. Electrochem. Soc. 151 (5) (2004) H117–H121.
[31] M. Shah, P.W. Voorhees, S.A. Barnett, Solid State Ionics 187 (1) (2011) 64–67.
[32] K. Yamahara, C.P. Jacobson, S.J. Visco, L.C. De Jonghe, Solid State Ionics 176 (5–6) (2005) 451–456.
[33] M.C. Tucker, G.Y. Lau, C.P. Jacobson, L.C. DeJonghe, S.J. Visco, J. Power Sources 171 (2) (2007) 477–482.